Hindawi
International Journal of Geophysics
Volume 2018, Article ID 5845670, 11 pages
https://doi.org/10.1155/2018/5845670

Research Article

Mapping of Deep Tectonic Structures of Central and Southern Cameroon by an Interpretation of Surface and Satellite Magnetic Data

Constantin Mathieu Som Mbang,[1] **Charles Antoine Basseka**,[1] **Joseph Kamguia**,[2,3] **Jacques Etamè**,[1] **Cyrille Donald Njiteu Tchoukeu**,[1] **and Marcelin Pemi Mouzong**[2,4]

[1]*Department of Earth Science, Faculty of Science, University of Douala, P.O. Box 24157, Douala, Cameroon*
[2]*Department of Physics, Faculty of Science, University of Yaoundé I, P.O. Box 47, Yaoundé, Cameroon*
[3]*National Institute of Cartography, Yaoundé, Cameroon*
[4]*Department of Renewable Energy, Higher Technical Teachers' Training College, University of Buea, P.O. Box 249, at Kumba, Cameroon*

Correspondence should be addressed to Constantin Mathieu Som Mbang; s_1blessing@yahoo.fr

Received 29 November 2017; Accepted 26 April 2018; Published 20 June 2018

Academic Editor: Filippos Vallianatos

The aim of this study is to determine the depth of deep tectonic structures observed in the Adamawa-Yadé zone (central part of Cameroon) and propose a new structural map of this area. The horizontal gradient associated with upward continuation and the 3D Euler deconvolution methods have been applied to the Earth Magnetic Anomaly Grid 2 (EMAG2) data from the study area. The determination of the maximum magnitude of the horizontal gradient of the total magnetic intensity field reduced to the equator, in addition to the main contacts deducted by Euler solution, allowed the production of a structural map to show the fault systems for the survey area. This result reveals the existence of two structural domains which is thus confirmed by the contrast of magnetic susceptibility in the Central Cameroon Zone. The suggested depths are in the range of 3.34 km to 4.63 km. The structural map shows two types of faults (minors and majors) with W-E, N-S, NW-SE, NE-SW, ENE-WSW, WNW-ESE, NNE-SSW, and NNW-SSE trending. The major faults which are deepest (3.81 km to 4.63 km) with NE-SW, W-E, and N-S direction are very represented in the second domain which includes the Pangar-Djerem zone. This domain which recovers many localities (Ngaoundéré, Tibati, Ngaoundal, Yoko Bétaré-Oya, and Yaoundé) is associated with the Pan-African orogeny and the Cameroon Volcanic Line.

1. Introduction

The study area is located in the central part of Cameroon (Central Africa) between 11°30′00″E and 15°30′00″E and between 3°00′00″N and 7°30′00″N (Figure 1). This area, with an average altitude of 1200 m, occupies the Adamawa High relief and the southern plateau of Cameroon. The area of study is part of the Precambrian formations (central and southern parts of Cameroon), which is represented by the Congo craton. The study area has been affected by many series of tectonic activities due to the collision between the Pan-African belt and the Congo craton. According to geological studies, the Pan-African domain was formed during the Pan-African event in late Proterozoic to early Palaeozoic by convergence and collision between the Congo craton to the South and the Pan-African mobile belt to the north [1]. Magnetic studies by [2] characterize the presence and the depth of granitic intrusion into the metamorphic formations in Akonolinga-Mbama region. Reference [3] proposed a structural map of the Southeast Cameroon. They mark out deepest accidents with depth about 3000 m to 4000 m and NW-SE direction. Reference [4] characterized three structural domains in the Southern Cameroon and detected in the Congo craton, the faults which extend over 400 km among Cameroon to Central African Republic (CAR) with W-E, NE-SW, and ENE-WSW direction. Our work consists of using horizontal gradient associated with upward continuation and 3D Euler deconvolution methods to delineate the deepest

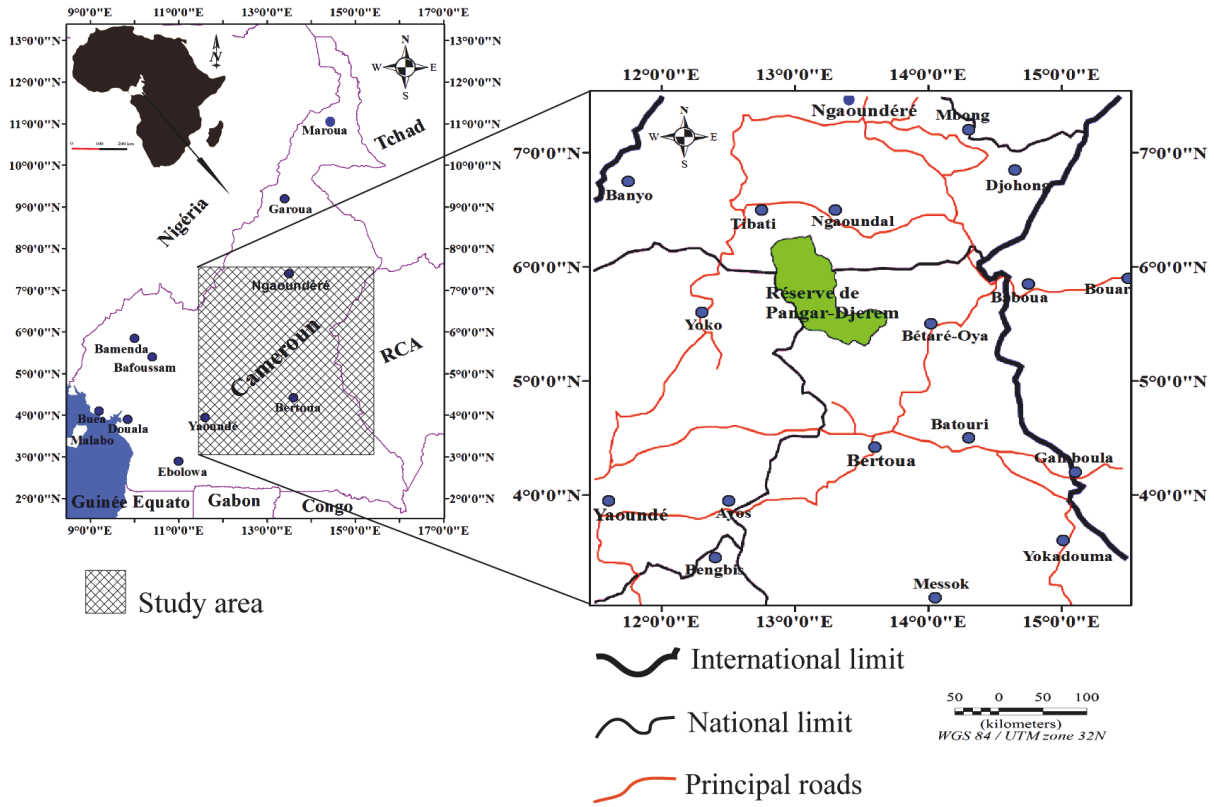

Figure 1: Localization of the study area.

faults and proposing a new structural map of the central part of Cameroon.

2. Geology and Tectonic Setting

The study area is located to the SE part of the Tibati-Banyo Fault (TBF). It is partly combined of the Central Zone and Southern Zone of Cameroon which extends from the southern of TBF to the northern limit of Congo craton. It contains volcanic formations (Cenozoic), Post-Pan-African formations, synt- to post-tectonic granitoid (600–500 Ma), Meso- to Neoproterozoic formations (1000-700 Ma),and paleoproterozoic gneiss (2100 Ma).

The geologic context of the study area (Figure 2) takes place at the North-Equatorial Pan-African Chain (NEPC) and the Congo craton (Ntem Complex). The area presents predominance of Precambrian formations of the Adamawa-Yadé zone [5–10]. These formations are organized in the Yadé massive, Lom group, and rocks of base complex.

In the western part of CAR (between latitude $3^{\circ}00'00''$N and $8^{\circ}00'00''$N), the Yadé massive is marked by Precambrian rocks of date Proterozoic and a not well-known granito-gneissic complex of supposed Archean age [11]. Its proximity to Cameroon (at the level of Adamawa), the continuity of field structures, and the isotopic studies Sm-Nd [1] leaves the thought that the Yadé massive rests on paleoproterozoic crust which suggests that the latter will be an extension of the Central Cameroon Sector.

The Lom group (West of the Sanaga basin) is a narrow belt of discontinuous and discordant rocks on the previous (gneiss and migmatites) of the basement complex [10]. It is composed of ancient continental sedimentary formations, probably constituted of shale, sand, marl, and arkose. These sedimentary deposits have undergone weak regional metamorphism which permitted the transformation of schist to seritoschists, chloritoschists, graphitic schists, sandy schists, and quartzites, to coarse grained conglomeratic quartzites, to quartzite of medium grained, fine-grained quartzites and to differentiate the phyllitic and siliceous facies. In the Lom valley, these metamorphosed volcano-sedimentary formations form a large band oriented NE-SW. With a sigmoidal form, it extends to 200 km of length and about 10 km to 30 km of width, at the Center of West Cameroon till the CAR covering a surface of 2500 km^2.

The basement complex constitutes the cristallophyllites rocks (Ectinites and Migmatites) corresponding to the ancient sediments probably marine, associated with ancient eruptive and intrusive rocks represented by syn to post-tectonic granites.

The Ectinites which correspond to inferior gneiss are very present at the boundary of Adamawa and the South of Batouri. The geological features encountered are as follows: gneiss to garnet, gneiss to amphiboles, leptynites, leptynites garnetified, and garnets.

Migmatites are observed in north of Yaoundé, Bafia, Foumban, Banyo, Tibati, and south of Batouri. It represents

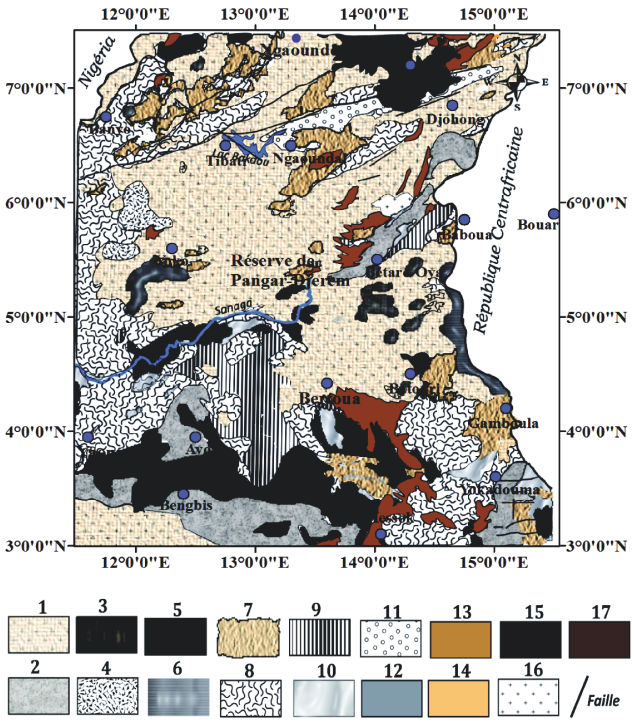

Figure 2: Geological map of the study area ([5] E: 1/1000000): 1, anatexite granite; 2, schist; 3, mica schist; 4, syenite; 5, tray basalt; 6, syn-tectonic granite (Monzonitic, discordant with biotite); 7, anatexite or migmatite with biotite); 8, embrechite gneiss; 9, Upper gneiss (grenatifere with two micas); 10, quartzite (Lom group, Mbalmayo-Bengbis, and Ayos); 11, Sedimentary formation of cretaceous; 12, upper mica schist with chlorite (Poli group); 13, low gneiss (with biotite, amphibole, pyroxene, sillimanite and hypersthene); 14, amphibolite (para- and ortho-: greenstones); 15, pelites; 16, post-tectonic granite (microgranite); 17, calcoalkaline orthogneiss.

accessory minerals identical to those of Ectinites. The migmatites are distinguished in embrechites and in anatexites of two micas, or at biotite and amphibole which are relative to the formations found at SE of Batouri [10].

The ancient eruptive and intrusive rocks are made of ancient syn-tectonic granites (630–620 Ma) intrusive in the paleoproterozoic. The late syn-tectonic granites (600–580 Ma) present with the ones before, similarities specially in their average composition which tends to be alkaline. Those granites are sometimes concordant and reveal in some areas xenoliths of ancient metamorphic rocks; they are massive and the most important ones are observed in the SE part of Sesse basin, between Yoko and Mankin [10].

Structural studies reveal that the area was affected by three deformation phases [1, 12, 13].

(i) The first (deformation D_1) is implementing a subhorizontal foliation generally transposed by the second in a straight fold to the horizontal axis. It is responsible for the development of S_1 cleavage or schistosity, L_1 lineation, C_1 shear, and P_1 folding.

(ii) The second phase D_2 is characterized by a regional foliation of NE-SW direction and a steep slope towards the SE or NW. This phase is associated with the development of granitoid intrusions syn-D_2. A subhorizontal lineation L_2 is equally noted (of NE-SW direction and dipping SW), L_2 lineation, S_2 schistosity, P_2 folds, and the C_2 shear markers. These markers indicate a sinister movement in the northern part of the domain, in relation to the Tcholliré-Banyo fault (FTB) [13, 14], and the dextral movement in the southern part, in relation to the Central Cameroon Shear Zone (CCSZ) and the Adamawa fault [15, 16].

(iii) The deformation D_3 is marked by set of C_3 shear zones and P_3 folds.

Those different orogenesis phases have affected the study area, such as a multitude of tectonic structures (faults) which are linked to the shear zone at the Center of Cameroon and the Sanaga fault [17–19].

3. Data and Methods

3.1. Data. The global Earth Magnetic Anomaly Grid 2 (EMAG2) used in this study has been compiled from satellite, ship, and airborne magnetic measurements. EMAG2 is a significant update of the grid for the World Digital Magnetic Anomaly Map. The data were provided by the organizations listed at http://geomag.org/models/EMAG2/acknowledgments.html. The magnetic grid was obtained for four kilometres above the geoid with two-arc minute resolution [20]. Additional grid and track line data have been included, over both land and ocean. The data have been used to realize the Global Earth Magnetic Anomalies map which is the result of international collaboration based on the contribution of many suppliers in the world. The inclination and declination angles of the ambient field were taken as −13.271°N and −5.295°E, respectively (5.35°N, 13.5°E). The magnetic data were supplied by the acquisition contractor in UTM zone 32N (WGS84) coordinates. The numerical treatment of data was realized using *Geosoft Oasis Montaj 6.4.2* software package.

3.2. Methods. For this study, three methods were applied with the final goal of enhancing the signature of hidden lineaments. The location and estimation of magnetic contacts, associated with tectonic structures and other structural discontinuities, were achieved by the application of horizontal gradient associated with the upward continuation method. In this study, the residual map was obtained after an upward continuation of the TMI-RTE grids at 4 km. The residual of upward map at 4 km is used to realize the horizontal derivative map. In order to estimate and characterize source depths from gridded magnetic data, we applied the 3D Euler deconvolution method.

3.3. Horizontal Gradient Magnitude (HGM). The horizontal gradient magnitude (HGM) method is the simplest approach to identify areas of geological contacts sources of high susceptibility and determine tectonic structures. Generally, the horizontal gradient of magnetic anomaly which corresponds to a tabular body tends to overlie the edges of the body if the edges are vertical or horizontal and isolated from each other [21]. The main advantage of the horizontal gradient

method is its low sensitivity to the noise in the data because it only requires calculations of the two first-order horizontal derivatives of the field [22]. The HGM method is also good in delineating both shallow and deep sources. If M (x, y) is a point where the anomaly of magnetic field is located, the amplitude of the horizontal gradient magnitude [23] is expressed as follows:

$$\mathrm{HGM}(x, y) = \sqrt{\left(\frac{\partial M}{\partial x}\right)^2 + \left(\frac{\partial M}{\partial y}\right)^2} \quad (1)$$

where $(\partial M/\partial x)$ and $(\partial M/\partial y)$ are the horizontal derivatives of the magnetic data. This method is normally applied to grid data rather than profiles. The component x of the gradient accentuates discontinuities and the contacts in the N-S direction while the y component acts in similar way to the W-E direction. Once the TMI-RTE grid is upward continued at 4 km, the HDR filter is applied to the residual resulting in grid and local maxima are extracted.

The upward continuation processing of the residual map was obtained at various altitudes. The horizontal gradient maxima computation for each level was carried out. The progressive migration while increasing upward continuation height indicates the direction of features outlined [24–26]. The upward continuation is a separation technique of anomalies according to their nature. The method is used to separate regional anomalies to residual anomalies which are respectively associated with deep and shallow body sources. It is an analytical method that transforms and yields the response of a magnetic source body and gives the elevation above the original flight datum [27]. This transformation attenuates high frequency signal components associated with shallow magnetic sources and tends to underline deep regional-scale magnetic anomalies. The technique referred to as the multiscale horizontal derivative analysis has been applied to upward continued residual map of the Adamawa-Yadé zone or Central Cameroon area at four heights: 0.1 km, 0.3 km, 0.5 km, and 0.7 km.

3.4. 3D Euler Deconvolution. Reference [28] proposed a technique for analyzing magnetic profiles based on Euler's relation for homogeneous functions. The Euler deconvolution technique uses first-order x, y, and z derivatives to determine location and depth of various targets (sphere, cylinder, thin dike, contact), each characterized by a specific structural index. The technique was used to delineate geologic contacts, lineaments, or faults and estimate their depth. Euler deconvolution is commonly employed in magnetic interpretation because it requires only a little prior knowledge about the magnetic source geometry, and more importantly it requires no information about the magnetization vector [28, 29].

In the current study, the 3D Euler process is to produce a map showing the location and the corresponding depth estimations of geologic structures associated with magnetic anomalies in two-dimensional grid. The standard 3D Euler is based on solving Euler's homogeneity equation [29]:

$$N(B - T) = (x - x_0)\frac{\partial T}{\partial x} + (y + y_0)\frac{\partial T}{\partial y} + (z + z_0)\frac{\partial T}{\partial z} \quad (2)$$

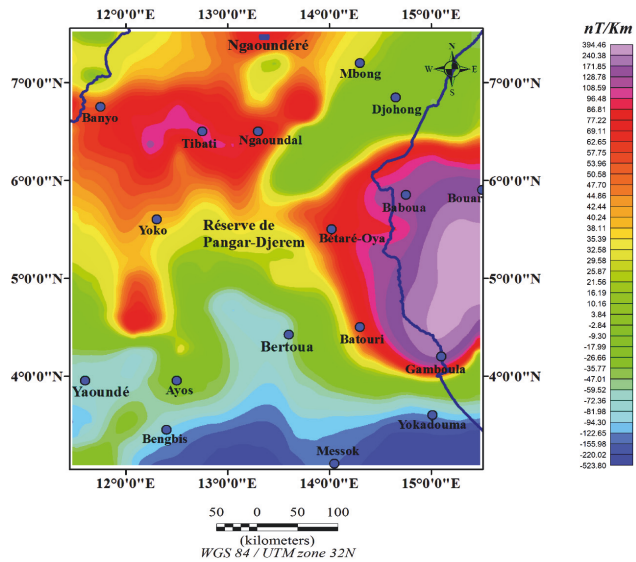

Figure 3: Total magnetic intensity map of the study area (TMI).

where $\partial T/\partial x$, $\partial T/\partial y$, and $\partial T/\partial z$ are the derivatives of the field in the x, y, and z directions, N is the homogeneity degree or structural index, B is the regional value of the total magnetic field, and (x_0, y_0, z_0) is the position of the causative source which produces the total magnetic field T measured at (x, y, z).

4. Results and Interpretation

4.1. Total Magnetic Map and Reduced Map to Equator (TMI-RTE). The total magnetic map (TMI) shows the variation of the magnetization field of the body buried under the ground (Figure 3). It is dominated by large anomalies (positive and negative) which are subcircular to linear, oriented NE-SW and W-E, with intensity between −523.80 *nT/km* and 394.46 *nT/km*. The anomalies with high positive values of order 108.59 *nT/km* to 394.46 *nT/km* are located between Tibati and Ngaoundal (general direction W-E), also between Bétaré-Oya, Batouri, Gamboula, Bouar, and Baboua (CAR) following NE-SW direction.

According to the intensity and orientation of these anomalies, the study area can be subdivided in two main domains.

(i) The first domain at the north between parallel $4°30'00''$N and $7°30'00''$N is constituted with positive anomalies located in Mbong and those which extend from Batouri to Bouar; Banyo to Ngaoundal and Ngaoundéré to the Pangar-Djerem reserve. The general direction of anomalies is NE-SW. These anomalies are concentrated on the Pan-African domain and can be correlated to the anatexite granites, ancient to late syn-tectonic granites, micaschists, granulites, schists, gneiss, migmatites, syenites, orthogneiss, basalts, amphibolites (para- and ortho-derivatives greenstones rocks), and cretaceous sedimentary formations.

(ii) The second domain at the south of the map underlines a large negative anomaly which extends over this area

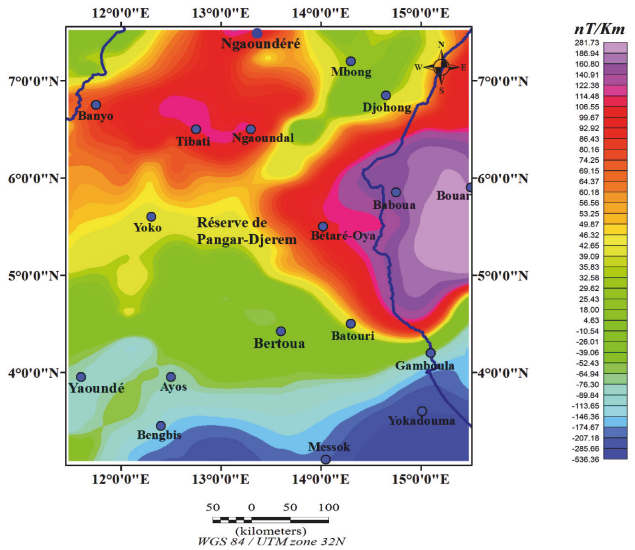

Figure 4: Total magnetic intensity map reduced to the equator (TMI-RTE).

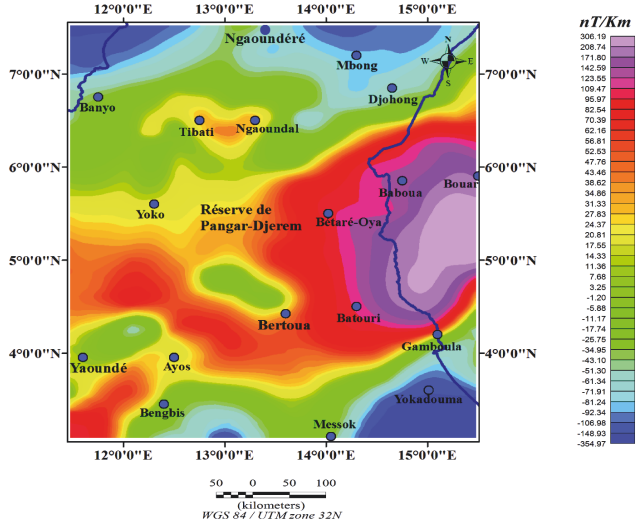

Figure 5: Residual map of TMI-RTE upward continued at 4 km.

following the meridian 11°30′0″E to 15°0′0″E and the parallel 3°00′00″N to 4°30′00″N. It plunges to the North of Bertoua with intensity between −523.80 *nT/km* and −47.01 *nT/km*. The major directions of the anomalies signatures deduced here are W-E and N-S. From West to East, it superimposes on the Pan-African and Archean formations constituted with gneiss, micaschists, schists, granites, quartzites, and migmatites.

The TMI map is characterized by high magnetic anomalies of NE-SW and W-E trending directions. This configuration may be attributed to relatively deep-seated low relief basement structures.

The RTE map (Figure 4) shows large anomalies, with virtually symmetric orientation NE-SW and W-E, of amplitude and shape close to that observed on the TMI. The intensity of those anomalies ranges from −536.36 *nT/km* to 281.73 *nT/km*. The first and second domains are easily identified and well delimited by positive anomaly (intensity 46.32 *nT/km*) which extends all the study area from East to West, passing through Batouri. A secondary anomaly which stakes the major is attenuated. This is tied to an eventual association of principal anomalies around the body having an induced behaviour. Thus, its magnetization may be probably due to two main reasons.

(i) The effect of the actual magnetic field

(ii) The fact that the parameters (declination and inclination) from the beginning are far from those which define the magnetization of the sources (in this present case will be remanent).

The positive anomalies are most amplified than those observed on TMI map. Their main direction NE-SW is preserved.

The negative anomalies are reduced compared to those of TMI map. This is remarkable at the level of Bertoua where the negative anomaly, well represented on the TMI, is not yet observed on the RTE.

4.2. Residual Map of TMI-RTE Upward Continued at 4 km. The TMI map is the result of the superposition of high and low effects of geological structures which correspond to regional and residual anomalies. To have a good correlation between anomalies and geological sources, it is necessary to separate these two components. The upward continuation is an analytical method used to separate a regional anomaly resulting from deep sources from residual anomaly due to shallow sources. The upward continuation with increasing heights highlights the magnetic effect of deep body sources because the transformation attenuates high frequency signal components associated with shallow magnetic sources and tends to underline deep regional-scale magnetic anomalies.

Figure 5 represents the area residual map of the TMI-RTE upward continued at 4 km. It is chosen like the reference level to characterize the behaviour of magnetic anomaly located in the study zone. Although differences are observed on this map, some previous observations made on the TMI-RTE map are still identified. The characteristic anomaly is observable between Tibati and Ngaoundal localities. Compared to the TMI-RTE maps, positive anomalies are better amplified from Yaoundé to Ayos and Batouri to Bouar. The residual magnetic map of our study region is characterized by moderate amplitude anomalies ranging between −354.97 *nT/km* and 306.19 *nT/km*. The general direction of anomalies is NE-SW. The negative anomalies recover the northern and south-eastern part of map respectively above rocks like basalts, granites, migmatites, schists, pelites, quartzites, and gneiss. In the central part, there is a large positive anomaly elongated NE-SW. This anomaly covers granites, schists, micaschists, migmatites, gneiss, and quartzites.

4.3. Horizontal Gradient. The horizontal gradient method is used to detect and interpret structural contacts regardless of their orientation. The method provides continuous contacts locations that are thin and straight. The HGM map of the study area has been realized by using the residual map of

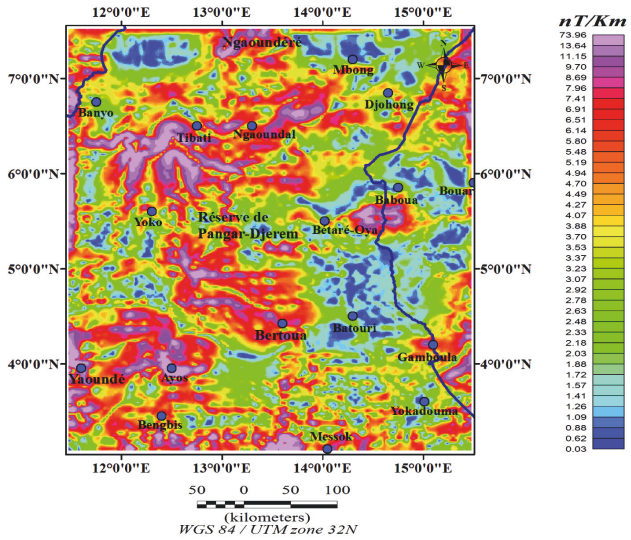

Figure 6: Horizontal gradient magnitude of TMI-RTE map upward at 4 km.

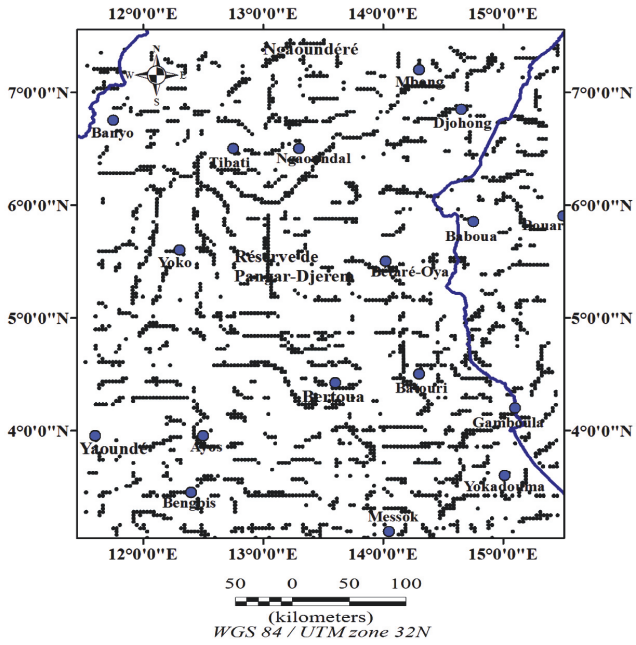

Figure 7: Maxima of the horizontal gradient magnitude map upward at 4 km.

the TMI-RTE upward continued at 4 km (Figure 6). The amplitude of gradient reaches 73.96 *nT/km*. The map shows majors anomalies in W-E, NE-SW, and NW-SE directions. The anomalies which were characterized with a large magnetic susceptibility are elongated and correspond to tectonic structure. From the south to the north, two anomaly domains are identified. The first domain which extends between the south of the map to the parallel 5°00′00″N shows the anomalies which are elongated W-E. These anomalies are located in Yaoundé, Ayos, and Bertoua. The second domain which includes the Pangar-Djerem reserve extends from 5°00′00″N to 7°30′00″N. In this part, the anomalies are located between the north of Yoko to the northern part of Ngaoundal with an extension observed in the NE of the map; they are mostly elongated NE-SW.

However, to highlight the contact direction represented on the HGM map, it is necessary to show the maxima of the HGM which is represented on Figure 7.

The maxima of the HGM reveal structural complexity such as faults inside the study zone.

According to the orientation of these maxima, two structural domains were recognized within the survey area.

(i) The southern domain (3°00′00″N to 4°30′00″N) where major lineaments are characterized by W-E trend. This domain which is geologically distinct to Congo craton formations was affected by Eburnean orogeny.

(ii) The northern domain located between 4°30′00″N and 7°30′00′N reveals four major directions (W-E, N-S, NE-SW, and NW-SE) of supposed faults. This multitude direction proofs that the northern part of our area of study which corresponds to the Pan-African mobile zone in Cameroon has been affected by significant tectonic activities during the Pan-African orogeny.

4.4. Multiscale Analysis of Gradient Maxima and Lineaments Map of the Studied Area. The maxima of horizontal gradient of magnetic anomalies help to locate contacts associated with abrupt changes in susceptibility and the multiscale analysis of these maxima and involve the upward continuation. The maxima map of our study area (Figure 7) has been obtained by using the HGM which was realized through the residual map upward at 4 Km. The horizontal gradient maxima of the magnetic anomalies showed in Figure 7 exhibits most structure features as lineaments and fractures. The linear local peaks of HGM are trending in NE-SW, NW-SE, W-E, and N-S directions.

Multiscale peaks analysis is process of edge detection in potential field data which corresponds to the maxima gradient position. During the process, each location of gradient maxima is obtained across multiple heights of upward continuation. The total horizontal gradient map (Figure 6) is upward continued up to 4.7 km with a step of 0.2 km (Figure 8). At those different altitudes, the persistence of the maxima allows differentiating the contacts. So, the analysis of the HGM's maxima map reveals major and minor lineaments. The major lineaments are much represented between 4°00′00″N and 7°00′00′N and the minor lineaments recover the entire map.

4.5. 3D Euler Deconvolution. To estimate the depth of the deep structures, the Euler method is applied the RTE-TMI map. In the study area, the Euler deconvolution was carried out by using the Standard Euler 3D method of Geosoft package. The Standard Euler 3D method leans on Euler's homogeneity equation that relates the magnetic field and its gradient components; it also locates the source with the structural index. The location of contact boundaries and lineaments is realized with a window size of 10 km grid cells, a maximum distance acceptable of 20 km, a depth tolerance error of 15%, and a structural index N = 0.

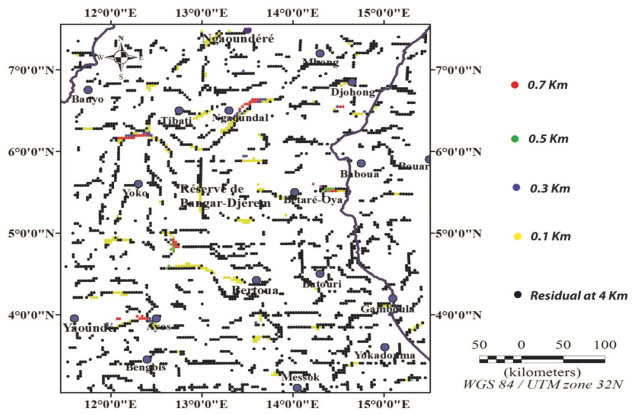

FIGURE 8: Maxima of the horizontal gradient of magnetic anomalies map upward continued to 4.1, 4.3, 4.5, and 4.7 km.

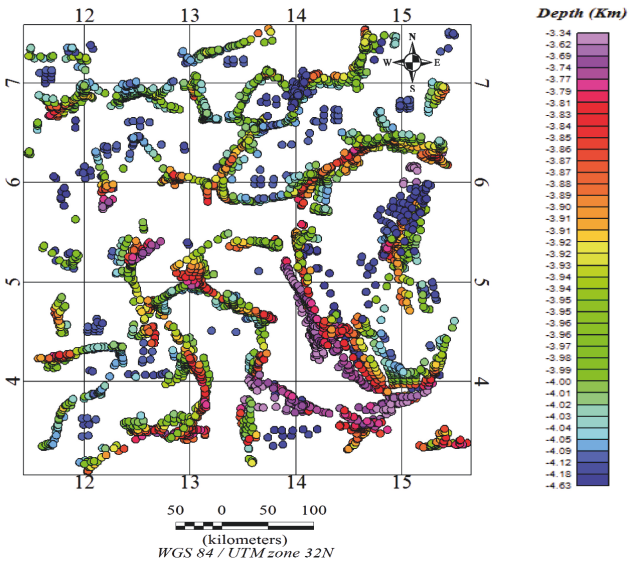

FIGURE 9: Euler depths map of the study area with geological boundaries obtained with structural index N = 0, window size of 10 grid cells, and depth tolerance of 15%.

The Euler solution map (Figure 9) obtained shows the different limits of geological structures which correspond to lineaments. The geological boundaries are marked out in NE, East, and Southern part, respectively, with NE-SW, NNE-SSW, and W-E trends. Furthermore, the map reveals the solutions for depths which are ranging between 3.34 and 4.63 km. In the central and the SE part of map, the Euler solutions show shallow depth of about 3.34 km to 3.89 km for the possible causative sources. In the eastern, the northern, and the SW part of the study area, the depths are not uniform. The two first parts are majority recover by depths about 4.63 km, and about 3.34 km to 3.9 km to the third part. In the NE part, the solutions are situated at depth of about 3.9 km to 4.63 km. The nonuniformity of the depths of those contacts suggests that all the outlines of the box do not have the same origin.

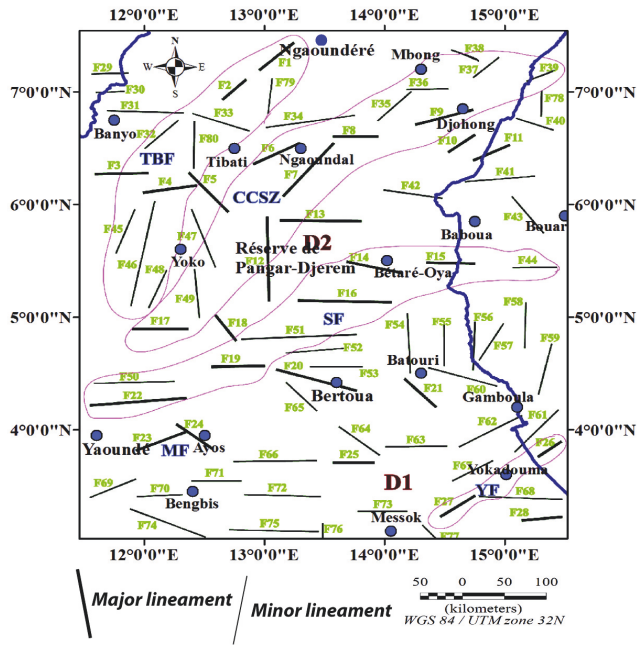

FIGURE 10: Magnetic lineaments map obtained for the study area showing the TBF, CCSZ, SF, YF, and MF or KF.

The Euler map given with coloured point shows the same main trends as the previous method (HGM). The output from the Euler method shows that there are many faults segments trending in W-E, N-S, NW-SE, NE-SW, and WNW-ESE directions.

The obtained results have permitted determining some deep tectonics structures. These different elements (lineaments) prove the presence of a probable deep contacts or geological boundaries.

4.6. Interpretation of the Structural Map. The observation of the structural map of HGM can be used to analyze direction trends of lineaments, which are even more observed in the Euler solution map. The magnetic data by horizontal gradient and Euler deconvolution methods were combined to produce the final interpretation of contact locations. The structural map of the study area (Figure 10) was traced by overlaying the maxima on the HGM upward continued at 4.7 km. The structural map obtained shows different features of our study area. These features show the structural complexity of the region which was distinct by magnetic anomalies with elongated shape. This proves that the basement rocks has been highly faulted and deformed. The deformation and faulting were result of the pronounced deformation and remobilization that occurred during the Pan-African orogeny about 600 to 500 ± 50 million years ago [30, 31]. Two types of lineaments (major and minor) have been identified. The major lineaments, materialized by bold black lines, are represented by the 28 first faults shown on Figure 10. They recover the western part of the area (at Yaoundé to Ngaoundéré including the Pangar-Djerem reserve) with general NE-SW trending which corresponds to the Cameroon Volcanic Line (CVL). We have highlighted in Figure 10, the Tibabi-Banyo

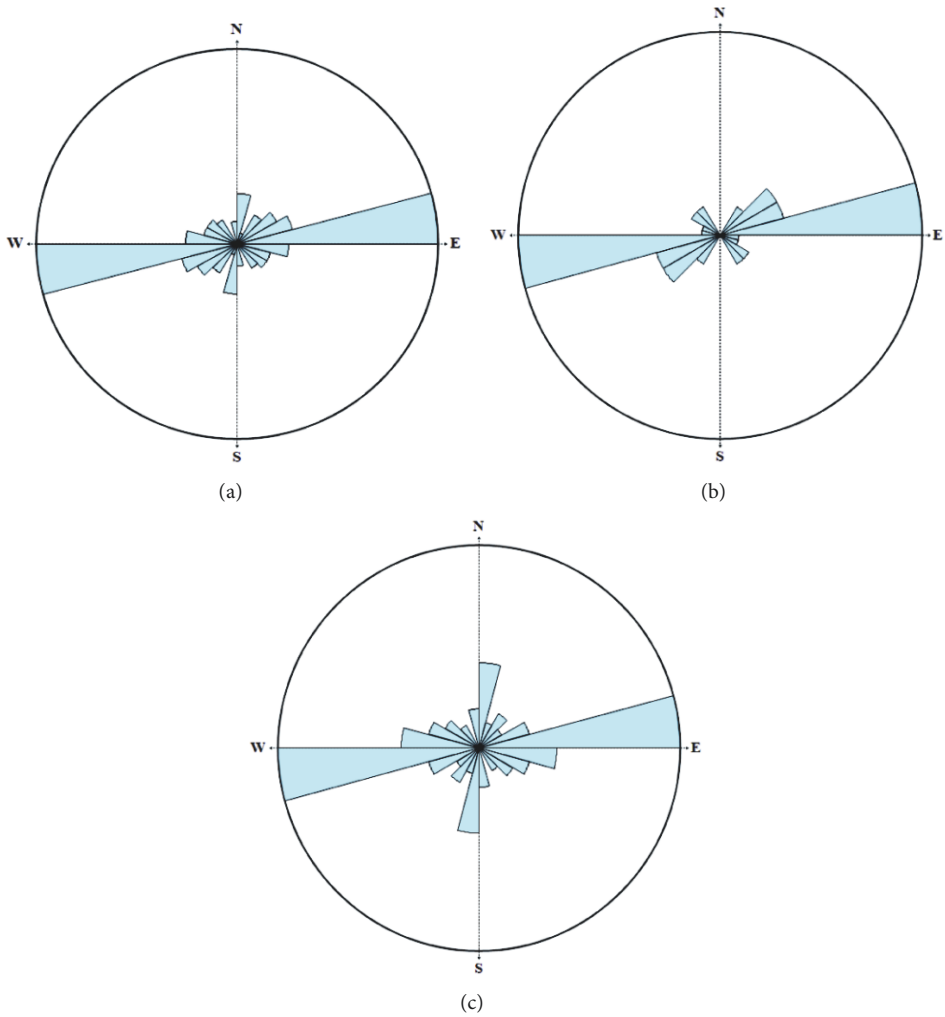

Figure 11: (a) Rose diagram of the general lineament orientations of the area studied; (b) rose diagram of the major lineament orientations; (c) rose diagram of the minor lineament orientations.

fault: F1, F2, F3, F4, F32, F33, F45, F46, F48, F79 and F80), the Central Cameroon Shear Zone (CCSZ: F6, F7, F8, F9, F12, F17, F35, F36, F37, F39 and F49), the Sanaga fault (SF: F14, F15, F16, F19, F22, F44, F50 and F51), the Mbalmayo fault (MF: F23 and F24) which can be interpreted as an extension of the Kribi fault (KF) extending to the SW to SE part of the study area; and the Yokadouma fault (YF: F26 and F27) corresponding to the deep fault detected in the SE Cameroon by aeromagnetic method [5]. In this part, the YF constitutes a tectonic junction with MF, Lobeke fault, and many other faults. The minor lineaments which correspond to the 52 other faults are mostly observed in the southern and eastern part of the study area. They extend at the southern to the northern part of the area and follow W-E, N-S WNW-ESE, and NW-SE directions. The results reveal the existence of two structural domains which are represented in the structural map by D1 and D2.

Table 1 gives the various directions of fractures that fit different lineaments observed on area study map.

The orientations of the lineaments extracted from the structural map (Figure 10) were displayed in a rose diagram program proposed by [32], to analyze the spatial distribution of lineaments, and the structural directions of our study area. Among the 80 extracted lineaments, 37.50% correspond to the largest trends in the W-E direction, 12.50% striking in the N-S direction, 11.25% also corresponding to NW-SE, NE-SW, and ENE-WSW direction. Another 16.25% correspond to WNW-ESE, NNE-SSW, and NNW-SSE directions. These proportions are represented in the general rose diagram (Figure 11(a)) which shows four major trends (W-E, N-S, ENE-WSW and WNW-ESE) of lineaments and four minor directions features with NE-SW, NW-SE, NNE-SSW, and NNW-SSE trends.

Figure 11(b) shows the different directions of major faults. The rose diagram of major faults trend reveals the presence of three important trends of lineaments. These directions are W-E, NE-SW, and ENE-WSW. The minor lineaments trends are represented on Figure 11(c). The major directions of minor lineament are W-E, N-S, and WNW-ESE.

Faults with N-S and W-E direction characterize the definitive stability of the Congo craton which would be

Table 1: Characteristic orientation of different fault segments.

Fault segment	Direction	Depth (km)	Fault segment	Direction	Depth (km)	Fault segment	Direction	Depth (km)
F1	NE-SW	4.0	F28	W-E	3.81	F55	N-S	3.81
F2	NE-SW	4.09	F29	W-E	3.81	F56	N-S	4.63
F3	W-E	4.63	F30	W-E	4.63	F57	NNE-SSW	
F4	W-E	4.09	F31	W-E	3.97	F58	N-S	3.97
F5	NW-SE	3.85	F32	NE-SW		F59	NNE-SSW	3.97
F6	ENE-WSW	4.63	F33	WNW-ESE	3.76	F60	WNW-ESE	4.14
F7	NE-SW	3.85	F34	W-E	4.05	F61	ENE-WSW	3.96
F8	W-E		F35	NE-SW	4.63	F62	ENE-WSW	3.97
F9	ENE-WSW	3.87	F36	W-E	3.74	F63	W-E	
F10	NE-SW		F37	NE-SW	4.63	F64	NW-SE	3.66
F11	ENE-WSW	3.87	F38	NW-SE		F65	NW-SE	3.92
F12	N-S	3.86	F39	ENE-WSW	3.92	F66	W-E	
F13	W-E	3.94	F40	WNW-ESE	3.62	F67	ENE-WSW	3.66
F14	WNW-ESE	3.93	F41	W-E	3.87	F68	W-E	3.74
F15	W-E	4.63	F42	WNW-ESE		F69	ENE-WSW	4.05
F16	W-E	3.88	F43	NW-SE		F70	W-E	
F17	W-E		F44	W-E	4.63	F71	W-E	3.95
F18	NW-SE	3.92	F45	NNE-SSW	4.63	F72	W-E	3.93
F19	W-E	3.95	F46	NNE-SSW	4.63	F73	W-E	4.63
F20	WNW-ESE	3.9	F47	NW-SE		F74	WNW-ESE	
F21	NW-SE	3.71	F48	NNE-SSW	3.34	F75	W-E	3.81
F22	W-E	3.71	F49	N-S	3.71	F76	N-S	3.92
F23	ENE-WSW	4.05	F50	W-E	3.94	F77	NW-SE	
F24	NW-SE	4.05	F51	W-E	3.74	F78	N-S	3.87
F25	W-E	3.66	F52	W-E	3.88	F79	N-S	3.62
F26	NE-SW	3.79	F53	W-E	3.97	F80	N-S	3.97
F27	NE-SW	3.87	F54	N-S	3.71			

associated with the Eburnean orogeny. The NE-SW and W-E trends represent the direction of tectonic structures associated with the Pan-African orogeny. The NE-SW and ENE-WSW directions are correlated with the direction of subduction of the Ntem Complex (cratonic plate) under the Pan-African mobile zone [3].

The interpretation of EMAG2 data using horizontal gradient associated with upward continuation and the 3D Euler deconvolution analysis methods has allowed identifying two structural domains. The two domains are located on the base complex which is associated with the Pan-African belt zone and the Ntem Complex or Congo craton. The results showed in Figure 10 prove that the second domain which is mostly characterized by major faults is located on the Pan-African belt zone. The general trend "NE-SW" of this domain is correlated with the trending of the Cameroon Volcanic Line. The minor faults in the southern part with W-E, N-S, and WNW-ESE trending materialized the stability of this domain which is represented by the Ntem Complex. The results observed here are in accordance with those obtained by [12, 33] who studied the Pan-African belt in Cameroon and proposed the lithostructural map of Cameroon. The lineament trends identified in the area are in accordance with the results obtained by [4] in the Southern Cameroon where the geological significance to the various anomalies and the highlighted structures of the subsurface formations have been marked out by [3] which had applied horizontal gradient, analytic signal, and the 3D Euler deconvolution methods to delineate the subsurface structures in the Southeast Cameroon.

The magnetic lineaments observed in our study area suggest that the area has been affected by an important regional field stress. The predominant W-E, N-S, NE-SW, ENE-WSW, and WNW-ESE fault directions prove that the regional stress field which affected the Base Complex in the Central Cameroon region is responsible for the reorientation of the former structures observed on the Ntem Complex or Congo craton [34].

The tectonic activity associated with the NW-SE and N-S predominant trending of magnetic lineament characterizes the stability of the Congo craton. The NE-SW and WSW-ENE directions are correlated with the direction of subduction of the Congo craton under the Pan-African [3].

The depth in the range of 3.34 km to 4.63 km is in accordance with the result of [3] in the Southeast Cameroon. Our result demonstrated that tectonic structures associated

with magnetic anomalies signature in the Adamawa-Yadé region were put in place during a major continental collision which correspond here to the collision between the Pan-African and the Congo craton (650-580 Ma; [1]).

5. Conclusion

The interpretation of magnetic anomalies of the Adamawa-Yadé zone between the Tibati-Banyo fault and the northern limit of the Congo craton has been realized by using EMAG2 data. Horizontal gradient associated with the upward continuation in addition with the 3D Euler methods has been used to filter magnetic data and enhance the data, the features that would be difficult to detect without outcrop and determine the depth of faults. Application of selected filtering methods to the magnetic data reveals the presence of deepest tectonic structures. The structural map obtained for the area is materialized by many faults with different directions which indicate a complex tectonic history and different phase of deformation. The major faults with direction trends W-E, NE-SW, N-S, NW-SE, and WNW-ESE are associated with the Cameroon Volcanic Line located in the Pan-African belt. The depths of these geological contacts or tectonic structures are estimated between 3.66 km and 4.63 km. The structural and tectonic elements obtained in our study area are also in accordance with those which were recently discovered by many authors using interpretation of aeromagnetic and EMAG2 data based on horizontal gradient, vertical gradient, upward continuation, analytic signal, and the tilt angle methods [3, 4].

Conflicts of Interest

The authors declare that they have no conflicts of interest.

Acknowledgments

The authors are grateful to the organizations listed at http://geomag.org/models/EMAG2/acknowledgments.html, for providing the EMAG2 data used in this study.

References

[1] S. F. Toteu, J. Penaye, and Y. P. Djomani, "Geodynamic evolution of the Pan-African belt in central Africa with special reference to Cameroon," *Canadian Journal of Earth Sciences*, vol. 41, no. 1, pp. 73–85, 2004.

[2] T. Ndougsa-Mbarga, D. Y. Layu, J. Q. Yene-Atangana, and C. T. Tabod, "Delineation of the northern limit of the Congo Craton based on spectral analysis and 2.5d modeling of aeromagnetic data in the Akonolinga-Mbama area, Cameroon," *Geofisica International*, vol. 53, no. 1, pp. 5-6, 2014.

[3] T. Ndougsa-Mbarga, A. Feumoé, E. Manguelle-Dicoum, and J. D. Fairhead, "Aeromagnetic data interpretation to locate Buried fault in South-East Cameroon," *Geophysica*, vol. 48, no. 1-2, pp. 49–63, 2012.

[4] C. A. Basseka, C. D. Njiteu Tchoukeu, A. Eyike Yomba, Y. Shandini, and J. V. Kenfack, "Apport des données magnétiques de surface et satellitaires à l'étude des structures profondes du Sud-Cameroun," *Sciences Technologies et Développement*, vol. 18, pp. 15–30, 2016.

[5] Ministère des Mines et de l'Énergie, *Carte géologique du Cameroun au 1/l 000 000 avec notice explicative*, 1979.

[6] J. Gazel and G. Gerard, "Carte géologique de reconnaissance du Cameroun au 1/500.000 coupure Batouri-Est avec une notice explicative de 50p," *Arch. De la Direction des Mines et de la Géologie du Cameroun. Yaoundé*, 1954.

[7] J. Gazel, M. Nickles, and V. Hourcq, "Carte géologique du Cameroun à 1/1000 000, 2 feuilles avec notice explicative," *Bull. Dir. Mines et Géol. Cameroun, n∘2 de la Direction des Mines et de la Géologie du Cameroun. Yaoundé*, 59 pages, 1956.

[8] M. Lassere, "Carte géologique de reconnaissance du Cameroun au 1/500.000 coupure Ngaoundéré-Est et Bossangoa–Ouest," *Notice explicative 50p. Dir. Mines et Géol. du Cameroun. Yaoundé*, 1962.

[9] A. Le Marechal, "Carte géologique de l'Ouest du Cameroun et de l'Adamaoua à 1/1000 000, 1 feuille avec notice explicative," *Service de cartographie de l'ORSTOM*, 1975.

[10] P. Dubreuil, J. Guiscafre, J. F. Nouvelot, and J. C. Olivry, "Le bassin de la rivière Sanaga : monographies hydrologiques," ORSTOM, n∘3. Paris, p. 11-18, 1975.

[11] J. L. Poidevin, "Les ceintures de roches vertes de la République Centrafricaine (Mbomou, Bandas, Boufoyo, Bogoin) : Contribution à la connaissance du Précambrien du Nord du craton du Congo," *Université Blaise Pascal de Clermont-Ferrand II*, 440 pages, 1991.

[12] S. F. Toteu, W. R. Van Schmus, J. Penaye, and A. Michard, "New U–Pb and Sm–Nd data from North-Central Cameroon and its bearing on the Pre-Pan African history of central Africa," *Precambrian Research*, vol. 67, no. 2001, pp. 321–347, 2001.

[13] R. Tchameni, A. Pouclet, J. Penaye, A. A. Ganwa, and S. F. Toteu, "Petrography and geochemistry of the Ngaoundéré Pan-African granitoids in Central North Cameroon: Implications for their sources and geological setting," *Journal of African Earth Sciences*, vol. 44, no. 4-5, pp. 511–529, 2006.

[14] A. A. Ganwa, W. Siebel, W. Frisch, and C. K. Shang, "Geochemistry of magmatic rocks and time constraints on deformational phases and shear zone slip in the Méiganga area, central Cameroon," *International Geology Review*, vol. 53, no. 7, pp. 759–784, 2011.

[15] T. Njanko, A. Nédélec, and P. Affaton, "Synkematic high-k calc-alkaline plutons associated with the Pan-African Central Cameroon shear zone (W-Tibati area): petrology and geodynamic significance," *Journal of African Earth Sciences*, vol. 44, no. 4-5, pp. 494–510, 2006.

[16] E. Njonfang, V. Ngako, M. Kwekam, and P. Affaton, "Les orthogneiss calco-alcalins de Foumban-Bankim: témoins d'une zone interne de marge active panafricaine en cisaillement," *Comptes Rendus de l'Académie des Sciences*, vol. 338, no. 9, pp. 606–616, 2006.

[17] J. P. Nzenti, P. Barbey, J. Macaudiere, and D. Soba, "Origin and evolution of the late precambrian high-grade Yaounde Gneisses (Cameroon)," *Precambrian Research*, vol. 38, no. 2, pp. 91–109, 1988.

[18] V. Ngako, P. Jegouzo, and J. P. Nzenti, "Le cisaillement Centre Camerounais. Rôle structural et géodynamique dans l'orogenèse panafricaine," *Comptes Rendus de L'Académie des Sciences de Paris, 313, série II*, pp. 457–463, 1991.

[19] V. Ngako, P. Affaton, J. M. Nnange, and T. Njanko, "Pan-African tectonic evolution in central and southern Cameroon: Transpression and transtension during sinistral shear movements," *Journal of African Earth Sciences*, vol. 36, no. 3, pp. 207–214, 2003.

[20] S. Maus, U. Barckhausen, H. Berkenbosch et al., "EMAG2: A 2-arc min resolution Earth Magnetic Anomaly Grid complied from satellite, airborne and marine magnetic measurements," *Geochemistry Geosystem*, vol. 10, article Q08005, 2009.

[21] L. Cordell, "Gravimetric expression of graben faulting in Santa Fe Country and the Espanola Basin, New Mexico," in *Proceedings of the Geological Society, Guidebook, 30th Field Conference*, pp. 59–64, Ingersoll, Raymond, 1979, http://nmgs.nmt.edu/publications/guidebooks/30.

[22] J. D. Phillips, "Processing and interpretation of aeromagnetic data for the Santa Cruz Basin-Patahonia Mountains area, South-Central Arizona," *U.S. Geological Survey Open-File Report 02-98*, 1998.

[23] R. J. Blakely and R. W. Simpson, "Approximating edges of source bodies from magnetic or gravity anomalies.," *Geophysics*, vol. 51, no. 7, pp. 1494–1498, 1986.

[24] M. L. C. Owona Angue, C. T. Tabod, S. Nguiya, J. V. Kenfack, and A. P. Tokam Kamga, "Delineation of lineaments in south cameroon (central africa) using gravity data," *Open Journal of Geology*, vol. 3, pp. 331–339, 2013.

[25] F. Koumetio, D. Njomo, C. N. Tatchum, A. P. Tokam, T. C. Tabod, and E. Manguelle-Dicoum, "Interpretation of gravity anomalies by multi-scale evaluation of maxima of gradient and 3D modeling in Bipindi region (South-West Cameroon)," *International Journal of Geosciences*, vol. 5, no. 12, pp. 1415–1425, 2014.

[26] Y. Shandini, J. M. Tadjou, and C. A. Basseka, "Delineating deep basement faults in South Cameroon area," *World Applied Sciences Journal*, vol. 14, no. 4, pp. 611–615, 2011.

[27] W. M. Telford, L. P. Geldard, R. E. Sherriff, and D. A. Keys, *Applied Geophysics*, vol. 860, Cambridge University Press, Cambridge, UK, 2nd edition, 1990.

[28] D. T. Thompson, "EULDPH: a new technique for making computer-assisted depth estimates from magnetic data," *Geophysics*, vol. 47, no. 1, pp. 31–37, 1982.

[29] A. B. Reid, J. M. Allsop, H. Granser, A. J. Millett, and I. W. Somerton, "Magnetic interpretation in three dimensions using Euler deconvolution," *Geophysics*, vol. 55, pp. 80–90, 1990.

[30] F. S. Toteu, "Chronologie des grands ensembles structuraux de la région de Poli," *Accrétion crustale dans la chaîne panafricaine du Nord Cameroun, thèse d'État, université Nancy 1*, p. 197, 1987.

[31] R. Trompette, "Neoprotérozoïc (600 Ma) aggregation of: western Gondwana a tentative Scenario," *Precambrian Researc*, vol. 82, pp. 101–112, 1997.

[32] A. Told and Thompson, "A Net 3.5 program to store, process, and display directional data," *Rose.Net. Version 0.10.0.0*, 2012.

[33] J. P. Nzenti, P. Barbey, J. Bertrand, and J. Macaudiere, "La chaîne panafricaine au Cameroun: cherchons suture et modèle," *Abstracts 15eme RST, Nancy, Société Géologique France, édition Paris*, p. 99, 1994.

[34] J. P. Vicat, "Esquisse géologique du Cameroun: in Géosciences au Cameroun," *Collection GEOCAM, 1/1998*, pp. 3–11, 1998.